AD NUMBER

AD477855

NEW LIMITATION CHANGE

TO

Approved for public release, distribution unlimited

FROM

Distribution authorized to U.S. Gov't. agencies and their contractors; Administrative/Operational Use; 24 AUG 1962. Other requests shall be referred to Navol Ordnance Laboratory, White Oak Center, Silver Spring, MD.

AUTHORITY

NOL ltr 15 Nov 1971

NOLTR 62-160

THEORETICAL CALCULATIONS ON THE SHOCK INITIATION OF SOLID EXPLOSIVES

24 AUGUST 1962

NOL
UNITED STATES NAVAL ORDNANCE LABORATORY, WHITE OAK, MARYLAND

NOLTR 62-160

(14) NOLTR-62-160

(6) THEORETICAL CALCULATIONS ON THE SHOCK INITIATION OF SOLID EXPLOSIVES

(9) Technical rept.,

(10) JULIUS W. ENIG and
FRED T. METCALF,

ABSTRACT: Theoretical calculations describing the initiation in heterogeneous TNT, RDX, Tetryl, Comp. B, Pentolite, and 75/25 Cyclotol produced by shocks up to 37 kilobars, are given. The "hot spot" initiation mechanism is simulated by using appropriate equations of state of the explosives and the resultant growth from shock to detonation wave is shown to be in qualitative agreement with experimental results. The shock wave in the explosive travels with increasing velocity due to the release of energy during chemical reaction in the neighborhood of the shock front, and then takes on a constant value upon reaching full detonation velocity. Numerical experiments show that the qualitative ordering of the sensitivity of the 6 explosives, based on one-dimensional gap test calculations, is the same as that obtained from the U.S. Naval Ordnance Laboratory experimental gap tests.

(11) 24 Aug 62.

(12) 30p.

P[redacted]

(17) NOL-FR-59

APPROVED BY: DONNA PRICE, Acting Chief
Physical Chemistry Division
CHEMISTRY RESEARCH DEPARTMENT
U.S. NAVAL ORDNANCE LABORATORY
WHITE OAK, SILVER SPRING, MARYLAND

This work was carried out under FR-59, Transition from Deflagration to Detonation. The results represent progress in theoretical treatment of this problem since the model chosen has qualitatively reproduced observed experimental trends.

R. E. ODENING
Captain, USN
Commander

Albert Lightbody
ALBERT LIGHTBODY
By direction

TABLE OF CONTENTS

INTRODUCTION

The processes occurring in the shock initiation of heterogeneous solid explosives are far more difficult to understand than those occurring in homogeneous liquids. The heterogeneous nature of the solid leads to neighborhoods of small local convergences in the shock wave pattern with the result that reaction takes place in these neighborhoods first. The energies released at these "hot spots" and the distribution and number of these hot spots then serve to determine the initiation characteristics of the explosive. A quantitative theoretical calculation taking these interactions into account presents a fluid flow problem so formidable as to be beyond the abilities of present methods and computers. Yet by lumping these interactions together so that the individual actions are lost but the qualitative effect of the whole remains, it is possible to derive results which are in excellent qualitative agreement with the experimental results. This is the purpose of this paper. A previous theoretical paper[1] has discussed the initiation of liquid explosives which show a behavior that is different from that of solids.

The large number of experimental investigations and more detailed explanations of the associated possible initiation mechanisms have been previously reviewed[2-7].

However, two experimental techniques will be briefly described here since the theoretical results reported in this paper are based upon a mathematical model which is taken as an approximation to the experiments.

An important explosive sensitivity test is the "gap test". Detailed descriptions of the test as used at the U. S. Naval Ordnance Laboratory are given elsewhere[8,9,10]. The experimental arrangement, as shown in Fig. 1, consists of a cylindrical donor explosive charge, a gap built up of an inert material, the cylindrical acceptor explosive charge whose sensitivity is to be determined, a small air gap, and a test plate. The donor (tetryl pellets) is caused to detonate through initiation by a detonator. A detonation wave propagates through the donor and subsequently a shock wave is transmitted into the gap. This shock wave, continuously attenuated by rarefaction waves from behind and from the sides, passes into the acceptor explosive and, if sufficiently strong, creates a temperature high enough to cause detonation. The energy stimulus in this case is the transmitted shock. A reaction strength comparable to detonation is indicated by a hole punched in the steel test plate. The donor charge material and dimensions are kept fixed and the length of the gap is increased or decreased until that critical length d_{50}, called the "50% gap value" or

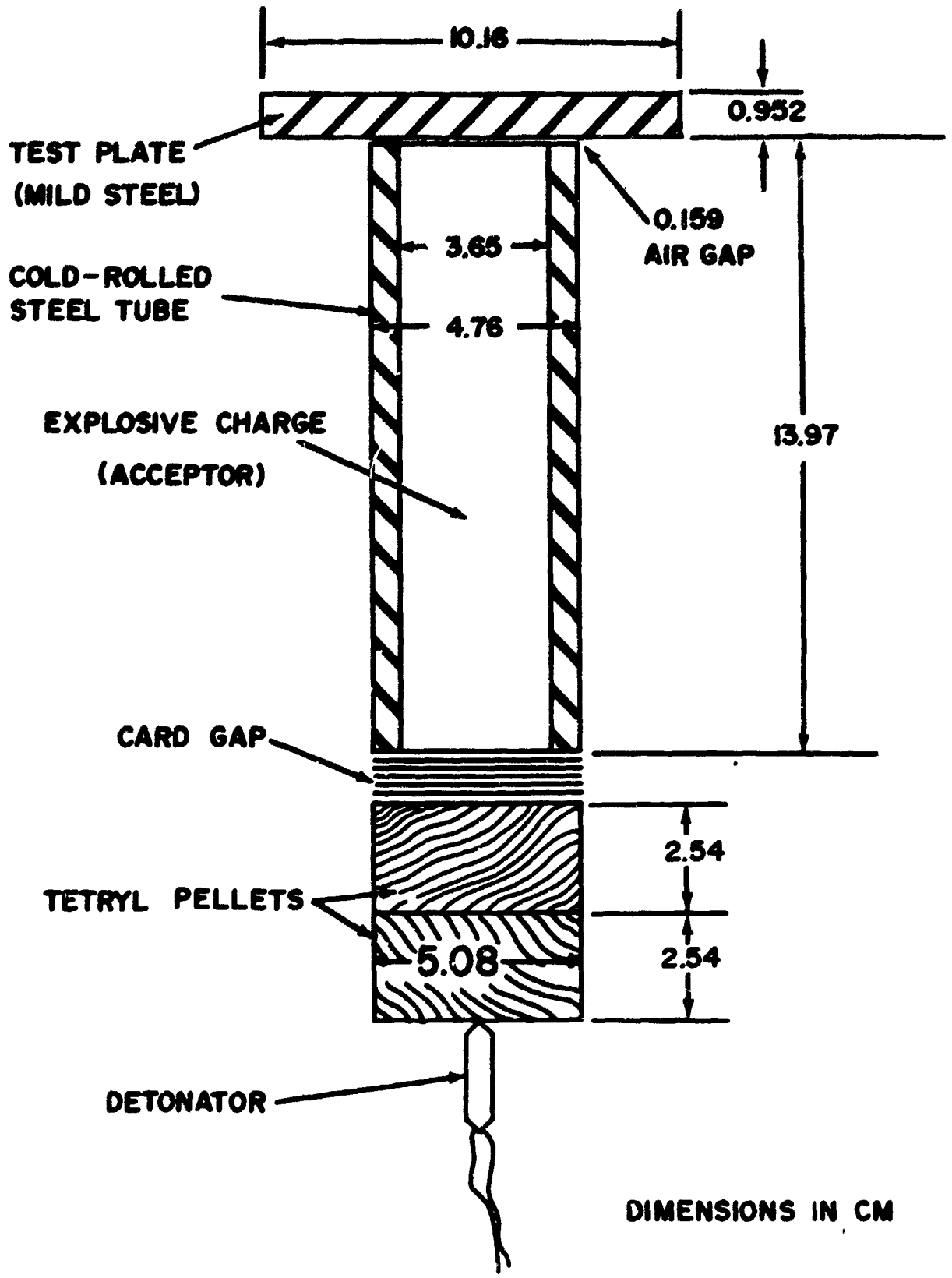

FIG. 1 THE NOL GAP TEST

"50% point", is reached such that further increase or decrease will cause the acceptor explosive always to fail to detonate or always to detonate, respectively. These 50% gap values, under carefully controlled conditions, are quite reproducible and remarkably sharp; statistical analysis of results from a 50 shot run on Comp B showed that the 50% point did not vary by more than a fraction of a millimeter[11]. On this sensitivity scale, the larger the 50% gap value the more sensitive the explosive. Smear cameras, high speed framing cameras, and electrical probes[12], and most recently, a conducting wire along the axis of the assembly[13] have been used to study the build-up from a shock wave to a detonation wave in the acceptor explosive[11]. The pressure of the initial transmitted shock in the acceptor explosive, that corresponds to d_{50}, is called the "initiating pressure" or the "50% pressure", P_{50}. The experimental gap test involves two-dimensional hydrodynamic flow since, for practical reasons, the characteristic diameter to donor + gap length ratio is not large enough to rule out the effect of lateral rarefaction waves on the amplitude of the shock when it enters the acceptor (even along the axis of symmetry).

A clever experimental technique, which minimizes troublesome two-dimensional effects in the shock initia-

tion of solid explosives, is the NOL wedge test developed by Jacobs[14]. Plane wave lenses are combined with additional high explosive and an inert shock attenuator to produce a shock wave of desired amplitude in the acceptor explosive. The acceptor explosive in the shape of a wedge is mounted as shown in Fig. 2 so that the progress of the shock or detonation wave can be seen as motion along the slant face. For fixed booster geometry, the thickness of the inert attenuator is varied until it is possible to discern a build-up of the shock velocity in the acceptor to detonation velocity. Various workers have postulated that this build-up is due to the continuous energy release behind the shock front brought about by chemical reaction. This technique has been further refined and used in the very extensive work of Campbell, et al[15]. Recent use of the wedge test to measure initiating pressures for Comp B-3 has resulted in values somewhat larger (ca. 30%) than those obtained in the gap test of Fig. 1[16].

The mechanism for the release of chemical energy behind the shock front in heterogeneous explosives is quite complicated and still poorly understood. But it is reasonable to attribute the difference between the initiation behaviors of homogeneous and heterogeneous explosives to the presence of voids and other defects in the latter. Experimental results for nitromethane[17] and nitromethane-

tion of solid explosives, is the NOL wedge test developed by Jacobs[14]. Plane wave lenses are combined with additional high explosive and an inert shock attenuator to produce a shock wave of desired amplitude in the acceptor explosive. The acceptor explosive in the shape of a wedge is mounted as shown in Fig. 2 so that the progress of the shock or detonation wave can be seen as motion along the slant face. For fixed booster geometry, the thickness of the inert attenuator is varied until it is possible to discern a build-up of the shock velocity in the acceptor to detonation velocity. Various workers have postulated that this build-up is due to the continuous energy release behind the shock front brought about by chemical reaction. This technique has been further refined and used in the very extensive work of Campbell, et al[15]. Recent use of the wedge test to measure initiating pressures for Comp B-3 has resulted in values somewhat larger (ca. 30%) than those obtained in the gap test of Fig. 1[16].

The mechanism for the release of chemical energy behind the shock front in heterogeneous explosives is quite complicated and still poorly understood. But it is reasonable to attribute the difference between the initiation behaviors of homogeneous and heterogeneous explosives to the presence of voids and other defects in the latter. Experimental results for nitromethane[17] and nitromethane-

carborundum mixtures[15] show that convergences in the mass flow and impedance mismatches can cause local reactions which have an important influence on the initiation process. For the mixture a detailed knowledge of the shock interactions is more important than a knowledge of the values of the thermochemical constants. It is well known that an explosive becomes easier to initiate as the density is decreased; and it is concluded that the increase in the number of voids leads to an increase in the number of hot spots formed, either through reactions occurring on the void surface, or through hot spots produced by shock convergence beyond the void. Recent computer calculations[18] describe the fluid flow resulting from a plane shock striking, from below, a bubble of vacuum suspended in nitromethane. The bubble is closed almost simultaneously everywhere because the lower surface has almost reversed itself by the time it hits the upper. The collapse is accompanied by the generation of a maximum temperature in the liquid, just above where the bubble had been; the temperature generated is at least twice that in the initial shock.

The experimental evidence indicates that in heterogeneous explosives the initial shock, which is too weak to raise the bulk of the compressed explosive to a temperature sufficient to cause reaction, creates hot spots where a small amount of energy is released and that this energy

production ceases soon after the shock front has passed over the particular hot spot. Furthermore, the compression waves originating at these centers of energy production continuously reinforce the shock, leading to eventual detonation at or near the front. Among others, Cachia and Whitbread[19] have experimentally determined the conditions under which the initial shock, instead of accelerating continuously into a detonation in the acceptor, decelerates and fades. In this case the reaction induced by the shock does not liberate sufficient energy to overcome the losses due to the rarefaction waves from the rear and sides. Retonation (detonation backwards through the partially reacted explosive) has been reported by some observers but not by others[15].

In this paper numerical experiments, based on a previously discussed computational scheme[1], are described in which a hot spot mechanism has been simulated in solid explosives and the resultant growth from shock to detonation wave is shown to be in qualitative agreement with experimental results. The hot spots are simulated by an appropriate choice of the equation of state, details of which are given in Section II. In Section III, the critical gap values and "50% pressures" derived from one-dimensional gap test calculations for TNT, RDX, Tetryl, Comp B, Pentolite, and 75/25 Cyclotol are compared with

experimental values and the initiation mechanism is discussed in detail.

II. EQUATIONS OF STATE

In the present calculations, the equations of state of unreacted explosive and product gas are similar to those previously used[1], i.e., for the explosive,

$$E_s = E_s^o + \left[(P+B)V_s - (P^o+B)V_s^o\right]/(\gamma_s-1), \tag{1}$$

$$E_s = E_s^o + c_{v,s}\,T + \left[AV_s^{1-\gamma_s} + (\gamma_s-1)BV_s/\gamma_s - (P^o+B)V_s^o\right]/(\gamma_s-1), \tag{2}$$

$$A = (V_s^o)^{\gamma_s}\left[P^o+B/\gamma_s-(\gamma_s-1)\,c_{v,s}T^o/V_s^o\right], \tag{3}$$

$$B = \rho_s^o(c_s^o)^2; \tag{3a}$$

and for the product gas,

$$E_g = PV_g/(\gamma_g-1), \tag{4}$$

$$E_g = c_{v,g}T, \tag{5}$$

where E,P,V,T, c_v, c, and ρ=1/V, are respectively, the specific internal energy, pressure, specific volume, temperature, specific heat at constant volume, adiabatic sound speed, and density; γ_s and γ_g are constants; and the subscripts g, s, and o refer respectively to product gas, unreacted explosive, and the initial state. If Q is the change in specific internal energy at P^o and T^o, i.e.,

$$Q = E_g(P^o,T^o) - E_g(P^o,T^o), \tag{6}$$

then substitution of Eqs. (2) and (5) into (6) defines E_g^o as

$$E_g^o = Q + c_{v,g}T^o. \tag{7}$$

The specific energy E and volume V for a mass cell of mixture are given by

$$E = wE_s + (1-w)E_g, \quad V = wV_s + (1-w)V_g, \tag{8}$$

where w ($o \le w \le 1$) is the mass fraction of unreacted explosive in the cell. The solid and gas in the cell are assumed to have the same instantaneous values of P and T. All the constants appearing in the equations of state for TNT, RDX, Tetryl, Comp B, Pentolite, and 75/25 Cyclotol are listed in Table I. The values of c_s^o for the 6 explosives were obtained from experimental shock data for TNT and Comp B[16] by interpolation on the initial densities in the P,u plane[20]; the values of γ_s were then obtained[21] from experimental values of P_{50}.

While the same form of the equation of state has been used for the solid explosive as previously[1] used for the liquid TNT, the values of γ are quite different ($\gamma = 3.178$ for liquid TNT). If T_1 is the temperature of the unreacted explosive, then the temperature along the

isentropic expansion curve from the state T_1, V_1 is given by

$$T = T_1(V_1/V)^{\gamma_s - 1}. \qquad (9)$$

Assuming now that only a small amount of reaction has already occurred before expansion, the temperature of the mixture can still be approximated by Eq. (9). For solids, values of $6.11 \leq \gamma_s \leq 7.12$ (see Table I) lead to much greater temperature increases during compression and decreases during expansion than for liquid TNT for the same relative increase or decrease in density. The result is that a rarefaction wave can abruptly quench reaction in a cell of such a solid explosive, whereas that same wave (same in the sense of having the identical instantaneous pressure-distance curve)may not quench reaction in liquid TNT. This has been verified in numerical experiments for both types of explosive.

As will be seen, the present choice of γ_s for the solid explosive does lead to effects which are qualitatively identical with those produced by hot spots. This equation of state, giving bulk temperatures which are too high for the compressions encountered in the gap test, simulates the high temperatures at the hot spots (which are surrounded by relatively cold explosive). Thus, the temperatures calculated here may be considered as the "hot spot temperatures". Likewise, the very large temperature

TABLE I PARAMETERS USED IN THE CALCULATIONS

Explosive[a]	ρ_s° g/cm³	P° bars	T° °K	c_s°[b] cm/μsec	γ_s[c]	a[b]	n kbar	$c_{v,s}$[ℓ] cal/(g deg)	Q[k] cal/g	E[ℓ] kcal/mole	z sec^{-1}	$c_{v,g}$ cal/(g deg)	γ_g
TNT	1.58[d]	1	300	0.227	6.68	2.119	81.4	0.5	984[d]	34.4[f]	$10^{11.4}$[f]	0.32	2.54[d]
RDX	1.59[d]	1	300	0.231	7.12	2.099	84.8	0.5	1228[d]	47.5[g]	$10^{18.5}$[g]	0.32	2.70[d]
Tetryl	1.63[d]	1	300	0.244	6.74	2.021	97.0	0.5	1047[d]	38.4[h]	$10^{15.4}$[h]	0.32	2.69[d]
Comp B	1.68[d]	1	300	0.259	6.29	1.929	112.7	0.5	1119[d]	47.5[i]	$10^{18.5}$[i]	0.32	2.74[d]
50/50 Pentolite	1.59[e]	1	300	0.231	6.99	2.099	84.8	0.5	1105[e]	39.5[j,m]	$10^{16.1}$[j,m]	0.32	2.64[e]
75/25 Cyclotol	1.70[d]	1	300	0.265	6.11	1.894	119.4	0.5	1167[d]	47.5[i]	$10^{18.5}$[i]	0.32	2.79[d]

a. TNT, RDX, and Tetryl are pure explosives; 75/25 Cyclotol is RDX/TNT, 75/25; Comp B is RDX/TNT/Wax, 60/40/1; Pentolite is PETN/TNT, 50/50.

b. See footnote 20 for method of calculation.

c. See footnote 21 for method of calculation.

d. Donna Price, Chem. Rev. 59, 801 (1959), see Table IV.

e. Donna Price, private communication.

f. A. J. B. Robertson, Trans. Faraday Soc. 44, 977 (1948).

g. A. J. B. Robertson, Trans. Faraday Soc. 45, 85 (1949).

h. A. J. B. Robertson, Trans. Faraday Soc. 44, 677 (1948).

i. RDX values used since RDX is the most sensitive component of the mixture.

j. The values for PETN in solution found by A.J.B. Robertson, J. Soc. Chem. Ind. (London), 67, 221 (1948), are used since PETN is the most sensitive component of the mixture.

k. The Q defined by Eq. (6) is the same Q of Table IV of Ref. c, where it is called the detonation energy.

ℓ. The estimates of J. Zinn and C. L. Mader, J. Appl. Phys. 31, 323 (1960) were used.

m. See footnote c of Table II.

decrease during expansion may be considered as the very large decrease in "hot spot temperature" due to the expansion occurring after the passage of the shock.

The inert gap material[22] is assumed to have a P,V Hugoniot curve given by

$$P = 58.4\ (0.847-V_G)/(0.272+V_G)^2\ ,$$

where P and V_G are in kilobars and cm^3/g, respectively; the isentropic expansion curve is assumed to follow the Hugoniot.

III. ONE-DIMENSIONAL GAP TEST CALCULATIONS

The calculations described below assume that the fluid flow is one-dimensional. While this is well approximated by the experimental wedge test, it is a rougher approximation for the experimental gap test, since here the pressure amplitude and the pressure distribution behind the shock, as it approaches the interface, has already been influenced by rarefaction waves from the sides.

In the explosive an irreversible first-order chemical reaction,

$$[s] \rightarrow [g]\ , \qquad (11)$$

is assumed, where the chemical kinetic equation which governs the conversion of unreacted solid explosive $[s]$ to product gas $[g]$ is

$$\partial w/\partial t = -Z\ w \exp\left[-E^{\ddagger} / (RT)\right]\ . \qquad (12)$$

Here, t, $E^{\ddagger}$, Z, and R are respectively, the time, activation energy, frequency factor, and gas constant. Values for $E^{\ddagger}$ and Z are given in Table I.

The calculational method involving the solution of the Lagrangean hydrodynamic equations, the equations of state, and Eq. (12) by finite differences is described elsewhere[1]. The number of mesh points used in these computations ranged from 110 to 150.

The one-dimensional idealized version of the gap test is shown in Fig. 3. A number of numerical experiments were performed in which the length of the donor explosive (Tetryl), d_{donor}, was fixed at 5.08 cm and the length of the inert gap d_G was varied until detonation in the acceptor explosive (TNT, RDX, Tetryl, Comp B, Pentolite, and 75/25 Cyclotol) was just barely possible. For larger gaps than this critical length d_G^*, detonation never propagated; for smaller gaps, detonation always propagated. The results of these machine computations (on an IBM 7090 computer) are given in Table II. Here $P_{crit.}$ and $T_{crit.}$ are the values of the pressure and temperature of the transmitted shock (as it entered the acceptor explosive) which correspond to d_G^*. In all cases, the shock initiated some reaction upon entering the acceptor explosive and had advanced a distance x_s into the explosive, continuously <u>increasing</u> in amplitude[23], at the time the explosive mass cell just

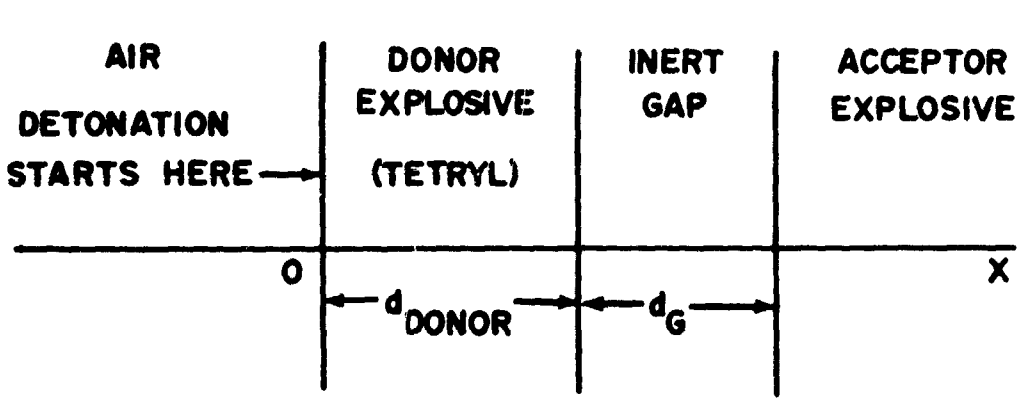

FIG. 3 IDEALIZED ONE-DIMENSIONAL GAP TEST

behind the shock front went to complete reaction. The values of d_Q^* and $P_{crit.}$ are compared, in Table II, with the experimental "50% gap values d_{50} and pressures P_{50}" obtained at the U.S. Naval Ordnance Laboratory with Lucite gaps[11]. However, the initial densities used in the calculations and those used in the experiments are different and are given in Table II. It is encouraging to note that although $P_{crit.}$ and P_{50} are quite different for some of the explosives, the relative ordering of the sensitivity of the explosives on the $P_{crit.}$ scale is the same as that on the P_{50} scale[24]. This is true not only for the pure explosives, TNT, RDX, and Tetryl, but also for the mixtures. The same ordering holds when comparing on the d_Q^* and d_{50} scales.

This theoretical model, with its numerous approximations, can be expected to reproduce experimental trends for series of pure explosives of appreciable differences in sensitivity. The fact that it also reproduces trends for the mixtures can be attributed, in part, to the sensitivity of the results to the choice of γ_s. This is shown most clearly for RDX and Pentolite; both had $\rho^o = 1.59$ and therefore, by the method used, the same Hugoniot. However, the respective ranges of $0 \leq P \leq 7$ and $0 \leq P \leq 11.8$ kbar resulted in γ_s values of 7.12 and 6.99. These, in turn, resulted in the <u>same</u> P_{crit} although the attenuation (d_Q^*)

TABLE II. Summary of calculational results. The explosives are listed in order of increasing sensitivity. x_s is the distance from the initial position of the interface to the shock front position where complete reaction first occurred (see Fig. 5). τ is the time interval between the time that the shock first entered the acceptor explosive and the time complete reaction first occurred at the shock front (see Fig. 5). $(\rho_s^o)_{exp}$ is the initial density of the explosive used in the experimental gap tests that yielded the values of P_{50} and d_{50} below.

Explosive [a]	ρ_s^o g/cm^3	P_{crit} kbar	T_{crit} °K	d_Q^* cm	x_s cm	τ μsec	$(\rho_s^o)_{exp}$ [b] g/cm^3	P_{50} [b] kbar	d_{50} [b] cm
TNT	1.58	37	930	25	7.3	15.2	1.62	37.3	3.5
75/25 Cyclotol	1.70	35	690	32	5.5	14.3	1.73	27.3	4.6
Comp B	1.68	31	680	39	3.8	9.1	1.70	21.3	5.1
Tetryl	1.63	26	706	53	3.1	7.6	1.62	11.8	6.6
Pentolite	1.59	19	667	68[c]	3.1		1.68	11.8	6.7
RDX	1.59	19	676	90	2.4	7.5	1.64	7.0	8.2

[a] TNT, RDX, and Tetryl are pure explosives; 75/25 Cyclotol is RDX/TNT, 75/25; Comp B is RDX/TNT/Wax, 60/40/1; Pentolite is PETN/TNT, 50/50.

[b] This information obtained from Ref. 11. All the explosives, except Tetryl and RDX, were cast. The standardized NOL gap test (Fig. 1 and Refs. 8,9,10) was used.

[c] The value of d_Q^* was computed from the $E^\ddagger$ and Z values for PETN of 39.5 kcal/mole and $10^{16.1}$ sec^{-1} respectively; they were obtained by Robertson (see footnote j of Table I) for decomposition in solution and are quite close to the values of Cook and Abegg [Ind. Eng. Chem. 48, 1090 (1956)] of 38.6 and $10^{15.3}$ found for the initial decomposition reaction. The first values tried in the present computation were 52.3 and $10^{23.1}$, those found by Cook and Abegg in a region of autocatalysis, and are comparable to Robertson's values of 47.0 and $10^{19.8}$ for decomposition of liquid PETN. The first computation gave a value of $d_Q^* > 110$ cm. and thereby resulted in an incorrect ordering of pentolite on the sensitivity scale.

differed by 22 cm of inert gap material. Of course, an additional difficulty in this case was the greater uncertainty of the proper values for $E^{\ddagger}$, Z, and Q of Pentolite.

The same sensitivity to γ_s is evident in the series of TNT, HMX and their mixtures, 75/25 Cyclotol and Comp B. Certainly it is to be expected that the cyclotol with 75% of the more sensitive component would be more sensitive than Comp B (about 60% HMX). Both experimental and computational results reverse the expected order. The reason for the reversal of the experimental results is probably lack of adequate control of physical variables such as particle size of the HMX. Indeed, recent carefully controlled tests of pressed charges have exhibited the expected sensitivity ordering[11]. The reversal of the computational results probably arises from the ranges used to derive γ_s and these in turn are based on the experimental results. It seems quite likely that repeating the treatment with use of the experimental results for pressed charges would reverse the order obtained with the cast charges reported here.

There seems little doubt that the present treatment can reproduce experimental trends for TNT, Tetryl, RDX, and their mixtures; a plot of $P_{crit.}$ vs. P_{50} is a smooth curve. The departure of the Pentolite result from this curve is attributed chiefly to the less adequate values of $E^{\ddagger}$ and Z for PETN.

The pressure distributions at various times for 75/25 Cyclotol are shown in Fig. 4; the other explosives show essentially the same profiles. In Fig. 4(a), the Taylor detonation wave has already reflected off the product gas - inert gap interface and a reflected rarefaction wave is moving back into the product gas, and a transmitted shock is moving into the gap. Only the rightmost part of the gas is shown since most of it is expanding to the left into a vacuum (approximating air at several bars). In Fig. 4(b) the progress of the shock in the gap is shown and in Fig. 4(c) the shock has reflected off the gap - 75/25 Cyclotol interface with the result that higher amplitude shocks are moving back into the gap and into the explosive. In Figs. 4(d) and 4(e), it can be seen that the pressure (and, therefore, temperature) of the transmitted shock is increasing because of chemical reaction behind the front (the reaction is apparent in the values of $w<1$ in the numerical solutions) although the rarefaction wave from the rear would tend to attenuate the shock. The pressure (and temperature) near the interface continuously decreases and, with this decrease, the chemical reaction abruptly ceases in contrast to the liquid TNT case[1] (where the temperature continues to rise). Here the temperature rises monotonically from the interface to the shock front and only in the neighborhood of the front is there appreciable chemical reaction. In Figs. 4(f) and 4(g), the

Fig. 4 The pressure distribution in the one-dimensional gap test for various values of t for 75/25 Cyclotol. The heavy vertical lines A, B, C, and D represent respectively, the air-product gas interface, the attenuator-75/25 Cyclotol (or product gas) interface, and the 75/25 Cyclotol-air interface. Each dot represents a mass point whose initial position is given by the Lagrangean coordinate x. The motion of any mass point in the X direction can be followed by observing the motion of that same dot (provided the observer has a pair of telescopic eyes). The values of t (μsec), as measured from the instant at which the shock first entered the explosive, are as follows: (a) -108.4, (b) -25.3, (c) -4.1, (d) 0.4, (e) 4.8, (f) 9.1, (g) 13.5, (h) 16.0, (i) 17.5, (j) 25.3.

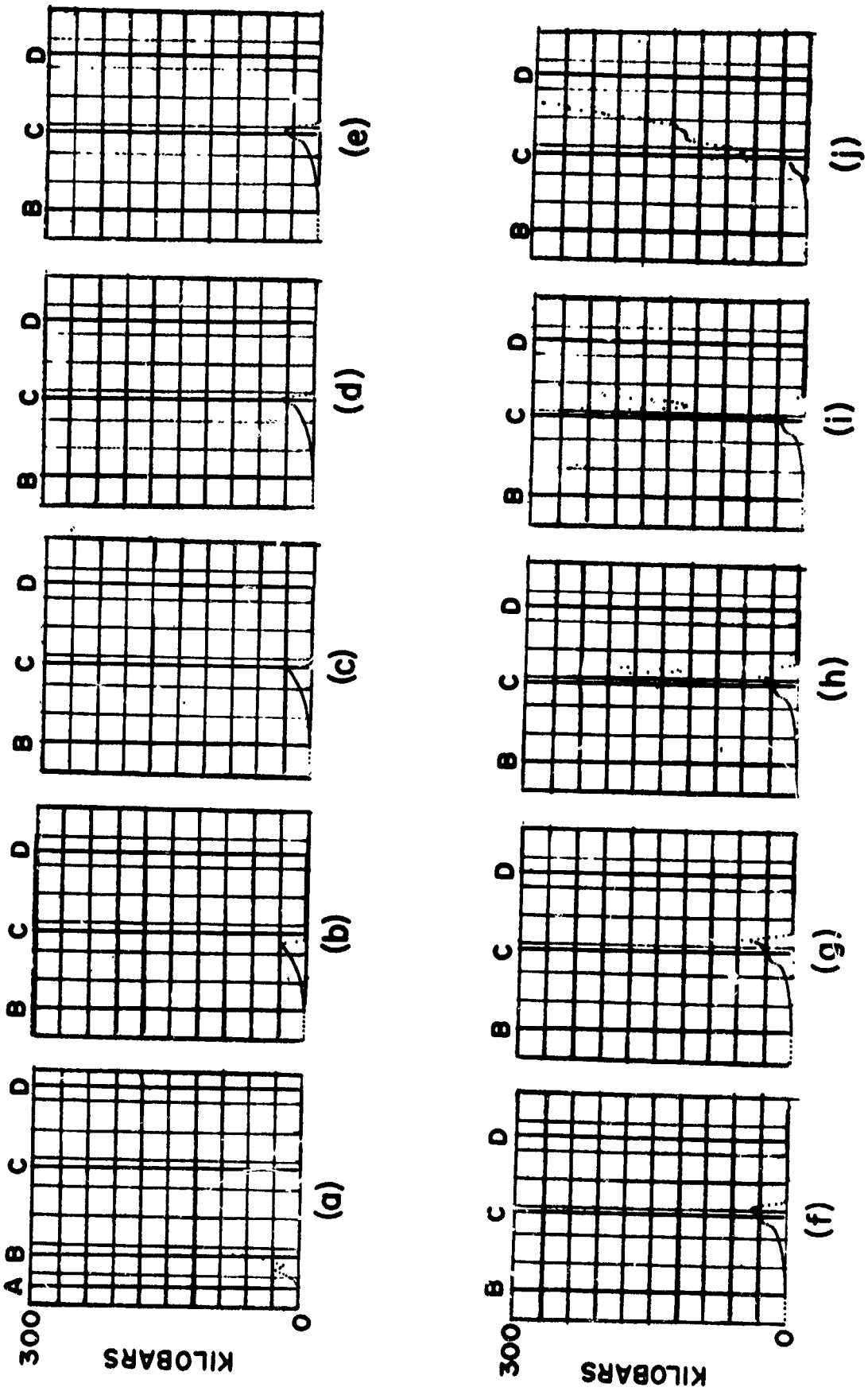

FIG. 4 PRESSURE DISTRIBUTION IN I-D GAP TEST FOR VARIOUS VALUES OF 1 FOR 75/25 CYCLOTOL

reaction is sufficiently rapid so as to lead to a rapid increase in pressure near the shock front. The transition to detonation is completed by Fig. 4(h). The detonation and retonation waves are shown in Fig. 4(i). Retonation completed, is shown in Fig. 4(j).

The t,X diagram is particularly informative for showing the wave and particle motion and this is depicted in Fig. 5 for 75/25 Cyclotol. Only motion in the vicinity of the gap-explosive interface is shown. The curve C_1 represents the motion of the shock wave in the gap before it strikes the gap-explosive interface. C_2 represents the path of the interface which moves with the local particle velocity while a transmitted shock wave moves along C_3 into the explosive, increasing in velocity from A to B. High-order detonation occurs just behind the shock front at B, and a constant velocity detonation wave advances along C_4. A retonation wave[25] starting at B moves through the partially reacted pre-compressed explosive along C_5 until it contacts the interface at D, where it gives rise to a transmitted shock that moves into the gap along C_6. Since the instantaneous temperature decreases monotonically from the shock front to the interface in the partially reacted pre-compressed explosive (and the temperature at the interface also decreases with time after passage of the shock), it is possible to find a curve C_7 which is the locus of points at which reaction is barely significant. Therefore, along lines of constant t to the left of C_7 the

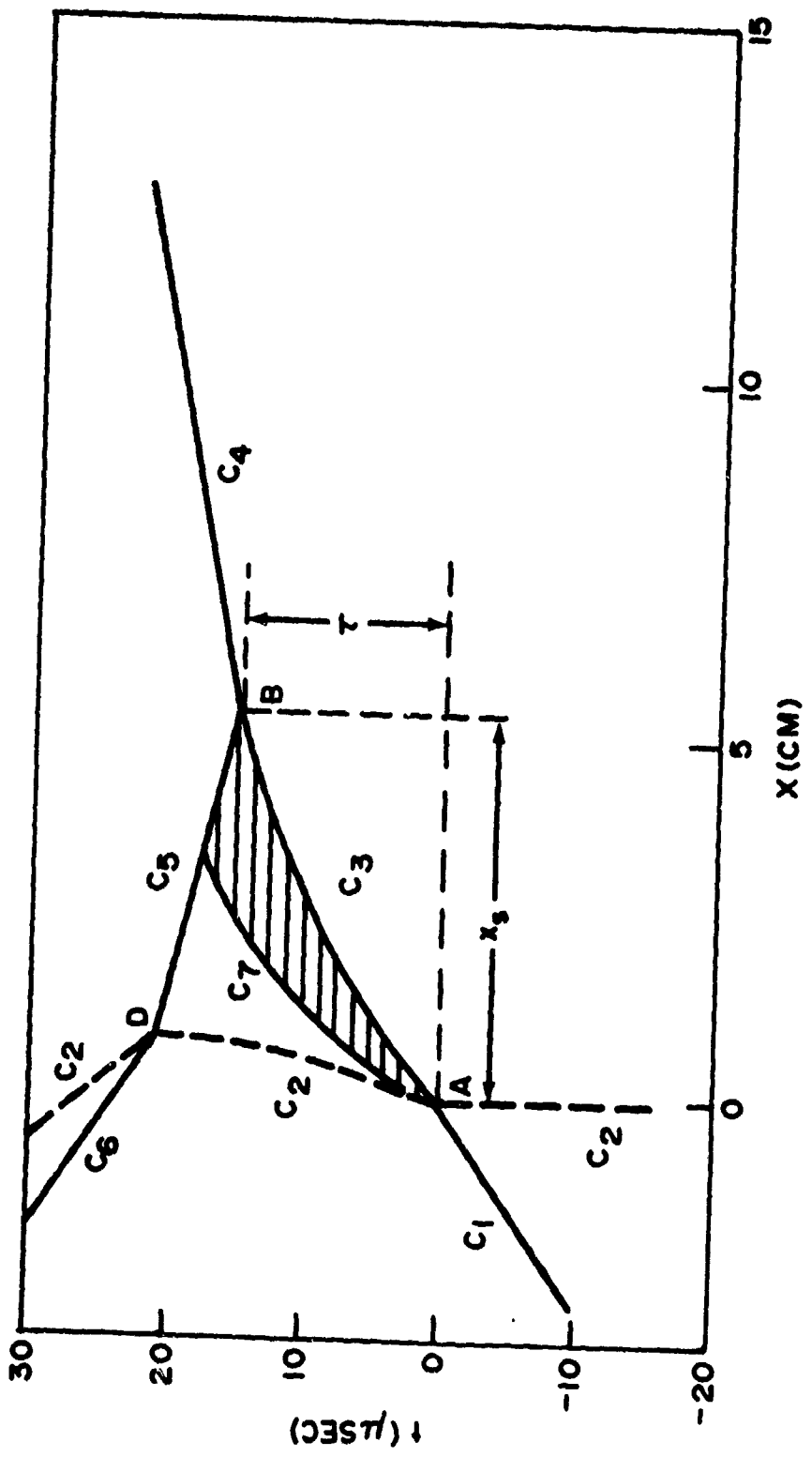

FIG. 5 t, X DIAGRAM SHOWING THE WAVE AND PARTICLE MOTION FOR CASE 2

reaction has essentially ceased (because T is too low), and to the right of C_7 reaction is significant. The lengths of the horizontal lines in the region between C_3 and C_7 represent the instantaneous widths of the reaction zones which supply an increasing amount of energy to drive the shock front along C_3. Thus, the model used for the above computations gives results which are in qualitative agreement with the hot spot theory of shock initiation of solid explosives. These hot spots are considered to be "active" and feeding chemical energy to the shock wave only for a short time after the shock wave has passed over them (and before the rarefaction wave from the rear has sufficiently cooled them). The hot spots may be considered to be distributed in the reaction zone that lies between C_3 and C_7. These time-dependent reaction zones are not to be confused with the steady state reaction zones; the latter, of course, are smaller.

ACKNOWLEDGEMENTS

It is a pleasure to acknowledge the debt of the authors to a number of people for their help, advice, and encouragement during the progress of this work. Most of them are members of the Chemistry Research and Explosions Research Departments of the U.S. Naval Ordnance Laboratory. The authors are particularly grateful to Dr. Donna Price for making available unpublished data, for critical review of

the results, for discussions which have been incorporated in this paper, and for other helpful suggestions.

Finally, the authors acknowledge with gratitude several very helpful suggestions from Dr. S. J. Jacobs.

REFERENCES AND NOTES

1 J. W. Enig and F. T. Metcalf, NOLTR 62-159, in press.

2 H. Eyring, R. E. Powell, G. H. Duffey, and R. B. Parlin, Chem. Revs. 45, 69 (1949).

3 F. P. Bowden and A. D. Yoffe, Initiation and Growth of Explosion in Liquids and Solids (Cambridge University Press, New York, 1952).

4 F. P. Bowden and A. D. Yoffe, Fast Reactions In Solids (Academic Press Inc., New York, 1958).

5 M. A. Cook, The Science of High Explosives (Reinhold Publishing Corporation, New York, 1958).

6 S. J. Jacobs, ARS J. 30, 151 (1960).

7 A. Maček, Chem. Revs. 62, 41 (1962).

8 A. B. Amster, E. C. Noonan, and G. J. Bryan, ARS J. 30, 960 (1960).

9 Donna Price and I. Jaffe, ARS J. 31, 595 (1961).

10 I. Jaffe, R. Beauregard, and A. Amster, ARS J. 32, 22 (1962).

11 Donna Price, I. Jaffe, and A. R. Clairmont, Jr., private communication.

12 See Ref. 6 for list of references.

13 R. W. Gipson and A. Maček, Eighth Symposium (International) on Combustion (The Williams and Wilkins Co., Baltimore, Maryland, 1962) 847.

14 This was used by Jacobs and Majowicz in 1955 and first reported in the open literature in J. M. Majowicz and S. J. Jacobs, Bull. Am. Phys. Soc. 5, 293 (1958).

15 A. W. Campbell, W. C. Davis, J. B. Ramsay, and J. R. Travis, Phys. Fluids 4, 511, (1961).

16 S. J. Jacobs, T. P. Liddiard, and B. E. Drimmer, in the preprints for the Discussion on Detonations of the Ninth International Symposium on Combustion, 1962, Cornell University.

17 A. W. Campbell, W. C. Davis, and J. R. Travis, Phys. Fluids 4, 498 (1961).

18 M. W. Evans, F. H. Harlow, B. D. Meixner, Phys. Fluids 5, 651, (1962).

19 G. P. Cachia and E. G. Whitbread, Proc. Roy. Soc. (London) A246, 268 (1958).

20 Let the subscripts 1 and 2 refer TNT and Comp B, respectively. From Ref. 16

$$U_i = c^{(i)} + a_i u, \quad i = 1,2 \tag{F1}$$

on their respective Hugoniots, where U and u are the shock and particle velocities respectively, and the $c^{(i)}$ and a_i are constants. For the initial densities $\rho^{(1)} = 1.615$ g/cm^3 and $\rho^{(2)} = 1.72$ g/cm^3, $c^{(1)} = 0.239$ cm/μsec, $c^{(2)} = 0.271$ cm/μsec, $a_1 = 2.05$, and $a_2 = 1.86$ Consider a test explosive of initial density ρ^o with an equation of state given by Eq. (1), and assume that at fixed u the shock pressure P can be found by a linear interpolation (or extrapolation) on the initial densities of TNT and Comp B, i.e.,

$$P = P_1 - (P_1-P_2)(\rho^{(1)}-\rho^o)/(\rho^{(1)}-\rho^{(2)}), \tag{F2}$$

where

$$P_i = \rho^{(i)}(c^{(i)}+a_i u)u, \quad i = 1,2 \tag{F3}$$

is obtained from Eq. (F1) and the Hugoniot relation,

$$P = \rho^{(j)} Uu, \quad j = 0, 1, 2 . \tag{F4}$$

The initial pressure P^o is always neglected in these calculations and the subscript s has been dropped. Substitution of Eq. (F3) in (F2) leads to

$$P = \rho^o(c^o + au)u, \tag{F5}$$

where

$$\rho^o{}_3{}^o = \left[\rho^{(2)}c^{(2)}(\rho^{(1)} - \rho^o) - \rho^{(1)}c^{(1)}(\rho^{(2)} - \rho^o)\right]/(\rho^{(1)} - \rho^{(2)}),$$

$$\rho^o a = \left[\rho^{(2)}a_2(\rho^{(1)} - \rho^o) - \rho^{(1)}a_1(\rho^{(2)} - \rho^o)\right]/(\rho^{(1)} - \rho^{(2)}). \tag{F6}$$

Eliminating P between Eqs. (F4) and (F5) gives

$$U = c^o + au \tag{F7}$$

for the test explosive. Thus $c_s^o \equiv c^o$ is known in Eq. (3a). Values of c_s^o and a are given in Table I.

[21] Eliminating E, P, and V between Eqs. (1), (F4) for j=0, and the other two Hugoniot relations,

$$E - E^o = \tfrac{1}{2} P(V^o - V), \tag{F8}$$

$$u^2 = P(V^o - V), \tag{F9}$$

leads to

$$\gamma = 1 - 2\left[1 - U/u + (c^o)^2/(Uu)\right], \tag{F10}$$

where the subscript s has been dropped. Obviously Eq. (F10) does not relate U linearly to u as demanded by Eq. (F7) if γ = constant. Therefore γ must be found such that the U,u curves of Eqs. (F7) and (F10) are reasonably close. Substituting Eq. (F7) into (F10) gives

$$\gamma = 1 + 2\left[a - 1 + ac^o/(c^o + au)\right], \tag{F11}$$

i.e., γ depends on u. From Eq. (F5) it is found that

$$2\,au = c^{o}(1+4aP/B)^{\frac{1}{2}} , \qquad \text{(F12)}$$

where the positive root has been taken. Using this value in Eq. (F11) yields

$$\gamma(P) = 1+2\left\{a-1+2a/\left[(1+4aP/B)^{\frac{1}{2}}+1\right]\right\} \qquad \text{(F13)}$$

The values of a and B given in Table I and the experimental "50% pressures" P_{50} listed in Table II are used to evaluate an average γ, $\gamma_{av.}$, over the Hugoniot pressure interval, $0 \leq P \leq P_{50}$, by means of the relation,

$$\gamma_s \equiv \gamma_{av.} = \tfrac{1}{2}\left[\gamma(0)+\gamma(P_{50})\right] . \qquad \text{(F14)}$$

For the six solid explosives considered, $\gamma(0)$ and $\gamma(P_{50})$ vary by at most 12% (TNT value) from γ_s, which is considered sufficiently accurate considering the approximations which have been made already.

[22] See footnote14 of Ref. (1).

[23] A similar increase in shock wave amplitude was obtained by M. H. Boyer (and others), Aeronutronic Systems Inc. (Ford Motor Co.), Pub. No. U-300, November 15, 1958, who used the very low values, $E^{\ddagger} = 46$ cal/g and $Z = 10^{8}$ sec^{-1}, which were calculated from the equation representing the adiabatic explosion time of a homogeneous explosive and the experimental delay times of Majowicz and Jacobs[14] for heterogeneous solid explosives. These low values greatly reduced the temperature sensitivity of the reaction rate.

[24] $P_{crit.}$ can easily be made to coincide with P_{50} by appropriately adjusting the value of γ_g, c_v, $E^{\ddagger}$, or Z, but then the purpose of the computations would be lost.

[25] Campbell, et al[15] find no retonation wave in their experiments and explain this by postulating a change in the hot spot characteristics of the partially reacted pre-compressed explosive. The model used in the numerical calculations cannot take these changes into consideration and therefore yields a retonation wave.